Damage Evolution and Energy Absorption of FRP Plates Subjected to Ballistic Impact Using a Numerical Model

L.J. Deka, S.D. Bartus and U.K. Vaidya
Department of Materials Science & Engineering
University of Alabama at Birmingham
Birmingham, AL 35294
e-mail: uvaidya@uab.edu, Phone: 205-934-9199

Abstract

High velocity transverse impact to laminated fiber reinforced composites is of interest in military and structural applications. Damage evaluation of the targets during impact based upon experimental work can be prohibitively expensive. However recent advances in the field of numerical simulation provide a means of predicting the performance characteristics of layered materials for ballistic protection. There is however, limited information about the ballistic response of reinforced thermoplastic composite materials. The overall objective of this work is to investigate the behavior of a plain weave laminated composites of varying thicknesses under high velocity impact both from an experimental and modeling view point. To analyze this problem, a series of ballistic impact tests have been performed on plain weave E-glass/polypropylene laminated composites of different thicknesses with a 0.50 caliber cylindrical shaped flat nose projectiles. A gas gun with a sabot stripper mechanism is employed to impact the panels. To analyze the perforation mechanism, ballistic limit and damage evaluation, an explicit three-dimensional finite element code LS-DYNA is being used. Selecting proper material models and contact definition is one of the major criteria for accuracy of the numerical simulation. During high velocity impact, composite laminates undergo progressive damage failure and hence, Material Model 161, a progressive failure model based on Hashin's criteria, has been assigned to predict failure of the laminates. The projectile is modeled using a Material Model 3 (MAT_PLASTIC_KINEMATIC). The laminates and the projectile are meshed using brick elements with single integration points. The impact velocity ranged from 187 to 332 m s^{-1}. A good correlation between the numerical and experimental results has been drawn in terms of predicting ballistic limit, delamination and energy absorption during impact.

Key words: Impact damage; composite laminates; energy absorption; numerical modeling

1. Introduction

Polymer matrix composite materials have realized steady increases in usage in many fields including aerospace, defence and automotive industries for structural and ballistic applications. The combined properties of individual constituent give them excellent specific strength and stiffness in addition to a high capacity to absorb kinetic energy. Fiber reinforced plastic (FRP) laminates are replacing structural light weight armor for advanced applications [1]. Composite laminates are comprised of multiple unidirectional or woven layers, bound together by a polymer matrix. During ballistic impact, kinetic energy of the projectile is dissipated through several mechanisms The predominant energy absorption mechanisms of laminates under high velocity, small mass impact are: kinetic energy imparted to the specimen, namely cone formation on the distal side of the laminate and/or spall formation, and energy absorption as a result of shear plugging, tensile fiber failure of the primary yarns, fiber debonding, fiber pull-out, elastic deformation of the secondary yarns, matrix cracking (intralaminar), interlaminar delamination, and frictional energy absorbed during interaction of the penetrator and laminate [2, 3, 4]. The two most prevalent experimental procedures for quantifying ballistic performance are V_B and V_{50}. The ballistic limit is defined as the velocity at which a projectile becomes embedded in the

specimen. The V_{50} is the velocity at which a projectile has a 50% chance of perforation with a deviation in velocity no greater than 40 m s^{-1} [5].

To increase the threat defeat level or to optimize the design of ballistic composite materials, material properties (strength and strain at high strain rates), failure mechanisms, type of threat, strain rate regime (e.g. low, intermediate, or high velocity) and laminate architecture must be known. Over the last several decades, a significant body of work has focused on experimental and theoretical research on the transverse impact response of polymer matrix composite laminates in order to gain insight into failure mechanisms and energy absorption. Most of the work to date has focused on thermoset composite systems [6-9] or high performance thermoplastic composite systems [10]. The focus of this work is to expand the knowledge-base on impact response of thermoplastic composite materials for ballistic protection.
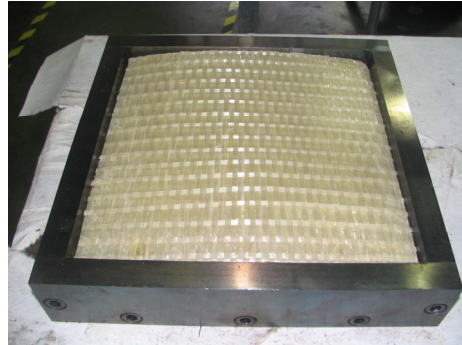
Wen [11, 12] investigated the perforation and penetration of FRP laminates using different projectile shapes, e.g. semi-hemispherical, conical, ogive and flat. He proposed analytical equations based on material properties and the static punch curve for each projectile geometry in order to predict the ballistic. Lee and Sun [7] evaluated the dynamic penetration of Carbon Fiber Reinforced Plastic (CFRP) laminates experimentally for a velocity range of 21- 91 m/s with a flat-ended cylindrical projectile. They defined the penetration process in three distinct stages; pre-delamination (fiber crushing), post-delamination before plugging, and post plugging. Mines et al. [6] studied transverse impact of E-glass/polyester laminates of different thicknesses with different projectile shapes. They found that the energy absorption mechanisms during penetration and perforation also exhibited the same behavior noted by Lee and Sun [7]. The exception being that shear plug formation is not usually seen in laminated glass composites.

A significant amount of work has focused on modeling failure mechanisms of composites subjected to transverse impact loading [13-19]. However, it is generally expected that composites fail in a progressive manner. Johnson et al. [20] reported a numerical method to predict composite damage using Continuum Damage Mechanics (CDM) suing the framework outlined by Ladevaze et al. [21-22]. Matzenmiller et al. [23] developed CDM model for unidirectional composites. On the basis of CDM, Williams and Vaziri wrote material subroutines for matrix/fiber failure in LS-DYNA [24]. Yen developed Material Model 161 (MAT 161) for LS-DYNA that captures the progressive failure mode of composite laminates (both unidirectional and plain weave laminates) during transverse impact. Because of its ability to model progressive damage, MAT 161 has been used successfully in predicting energy absorption and damage [25-27]. The objective of the current study is to model energy absorption and damage evolution in plain-weave thermoplastic composite laminates under transverse high velocity impact at/near V_B.

2. Experimental procedure

Polypropylene (PP) (BP Amoco 9965)/E-glass (Owens Corning 225 4588) 12 mm wide tapes and average thickness of 0.60 mm were produced using a hot-melt impregnation process. The were subsequently woven into a plain weave architecture and consolidated in 8, 12, and 16-layer laminates in a 30x30 cm^2 mold, Fig. 1, using a compression molding machine. This corresponded to average thickness of 5.25 mm, 8.15 mm and 11.00 mm, respectively. The consolidated material had an average fiber content of 67% weight (42% volume) and density 1585 kg m^{-3}.

A single-stage light gas gun consisting of a pressure chamber, a barrel and a nitrogen/helium tank was used to launch the projectiles. The impactor was a 0.50 caliber (12.7 mm) flat nosed cylinder made of alloyed tool steel with a mass of 13.40 g ± 0.03 g, which is consitant with the mass of a NATO 0.50 caliber Fragment Simulating Projectile (FSP). The projectile velocity was measured using photoelectric chronographs (Model: Oehler 35 and Oehler Sky Screens). The impact velocity was decreased from the full penetration condition to V_B or partial penetration condition in accordance with the V_{50} definition for the 8, 12, and 16 layer laminates, with four to five specimens in each test configuration.

3. Numerical Approach

3.1. Simulation Tools

Altair Hypermesh v7.0 and Finite Element Model Builder (eta/FEMB-PC version 28.0) were used in pre-processing. LS-DYNA (970) was used to analyze perforation mechanisms, failure modes, and damage evaluation during high velocity projectile impact of the PP/E-glass composite plates described in the previous section. The simulation cycle is shown in Figure 2.
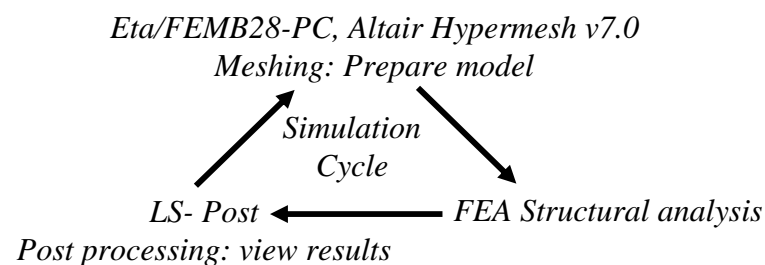
Eta/FEMB28-PC, Altair Hypermesh v7.0
Meshing: Prepare model

Simulation
Cycle

LS- Post ← *FEA Structural analysis*
Post processing: view results

Figure 2: Simulation cycle used in model development

3.2 Material model

Material Model 161 (MAT_COMPOSITE_MSC) was chosen for the impact simulation. MAT 59 (MAT _COMPOSITE_FAILURE _SOLID) is an orthotropic material model which uses maximum stress failure criterion. Once the maximum load is reached along a particular direction, the corresponding stiffness is set to zero in a time interval of 100 times steps. However, MAT 59 cannot predict delamination, and delamination plays a vital role in determining the impact performance. Unlike MAT 59, MAT 161 has the capability to model progressive damage under high strain rate and high pressure loading. MAT 161 is based on the Hashin's failure criteria

[28], which allows for five failure modes; tensile and compressive fiber failure, fiber crush, through-the-thickness matrix failure and delamination [29]. Criterion for element erosion is incorporated in MAT 161. This is crucial because during impact simulations, some elements in the impact region undergo large distortions, which may lead to numerical instabilities. Proper eroding criterion eliminates distorted elements without affecting the stability of the simulation.

The cylindrical projectile was modeled using Material Model 3 (MAT_PLASTIC_KINEMATIC). MAT3 is a bi-linear elastic-plastic model that contains formulations combining isotropic and kinematic hardening. In the present analysis, the hardening parameter was considered zero. More details on MAT 3, MAT 59 and MAT 161 can be found in Ref. [29].

3.3 Contact Type

Proper contact definition between projectile and the laminate is required to model high velocity transverse impact. Three different types of contacts between the impactor (slave) and the target (master) are adopted in LSDYNA; kinematic constraint method, the penalty method and the distributed parameter method. The segment based penalty contact (CONTACT_ERODING_SINGLE_SURFACE, SOFT=2) was defined for the contact between the projectile and the composite plate. This contact algorithm checks segment versus segment penetration and does not use the shooting node logic parameter because it ignores the initial penetrations. When segment penetration occurs, penalty forces are applied normal to the penetrating segment. These penalty forces are proportional to the excess penetration depth given by Equation 1:

$$f_{penalty} = K * \left(d_{current} - d_{initial} \right) \qquad (1)$$

where $f_{penalty}$ is penalty force, K is penalty stiffness, $d_{current}$ is the current penetration depth and $d_{initial}$ is the initial penetration depth. Here, the contact exhibits very little hourglass excitement due to the symmetry of the approach .But due to high pressure generation at the contact interfaces unacceptable penetration may occur. This can be avoided by scaling up the stiffness (SLSFAC) or scaling down the time step size [22]. In high velocity impact problems, the effect of frictional forces in interfaces is negligible. As the static friction (FS) should be greater than the dynamic friction (FD), FD was set at 0.1 while FS at 0.3.

3.4 Numerical model creation

As the damaged zone is of localized nature, the boundary conditions have little influence when impacted under ballistic regime. The composite plates and the projectile were meshed in Hypermesh™ using brick elements with single integration point (ELFORM= 1). The one point element is more robust than the fully integrated element (type 2, 3) in the case of large deformation. The dimension of the target was 15 x 15 cm^2 and number of layers used in each plate determined the target thickness. Each E-glass/PP layer had 1056 brick elements. The projectile which is cylindrical in shape with a blunt end was meshed with 2800 brick elements and assigned an initial velocity similar to the experimental condition. The modeled geometry and initial grid are shown in Figure 3. A very fine grid, relative to the plate boundaries, (brick element dimension (mm), 0.529 x 0.629 x 0.68) was used at the impact region of the target to obtain convergence and the grid dimension gradually increased to the outer edges, approximately up to 3.64 x 2.32 x 0.68 (mm). A coarser grid towards the edges leads to the failure of the aspect

ratio (>5). Failure of aspect ratio did not affect the numerical results as the impact region and its surroundings were discretized with very fine uniform brick elements. The interaction between the projectile and composite laminate was handled with erosion logic, using a gap size 0.01 mm and quarter symmetry approach was adopted for all the impact simulations to reduce the computational time. The material properties for the composite plate and the projectile used in the simulation are shown in Tables 1 and 2, while Table 3 provides the model dimensions.
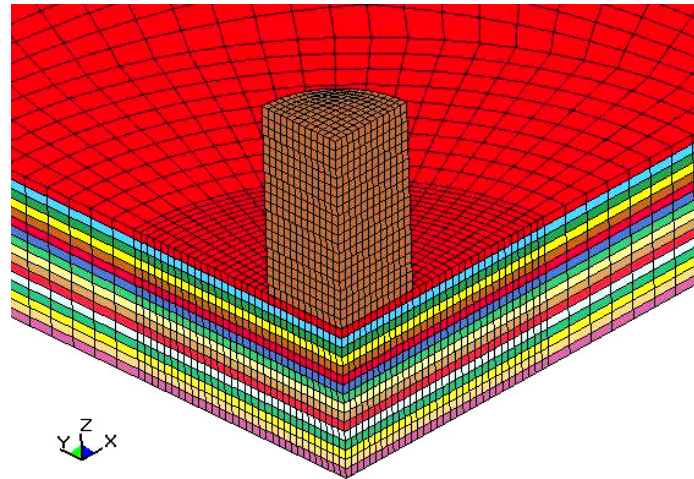

Figure 3: Quarter symmetry geometry of the projectile and 16 layer laminate.

Since the damage mechanisms in high velocity impact conditions are similar to those in quasi-static events, the strength properties of the PP/E-glass laminate were taken from quasi-static tests. Data related to strain rate sensitivity and erosion can be found in Ref [27]. The fiber mode crush strength and shear strength strongly affect the ballistic limit. It requires a lot of effort to get those test data from experiments. Due to unavailability of dynamic strength data, some of the strength parameters have been modified up to 10% to provide the best fit to the V_B of 16 layer composite plate.

Table 1.
Material properties for a plain-woven PP/E-glass composite layer

Density (Kg m^{-3})	ρ	1850
Young's modulus (GPa)	E_{11}	14
	E_{22}	14
	E_{33}	5.3
Shear modulus (GPa)	G_{21}	1.8
	G_{31}	0.75
	G_{32}	0.75
Poisson's ratio	υ_{21}	0.08
	υ_{31}	0.14
	υ_{32}	0.15
Tensile strength (GPa) *	X_T	0.45
	Y_T	0.45
	Z_T	0.15
Compressive strength (GPa) *	X_C	0.25
	Y_C	0.25
Matrix mode shear strength (Gpa) *	S_{12}	0.032
	S_{23}	0.032
	S_{31}	0.032
Fiber shear strength (GPa)	S_{FS}	0.3
Fiber crush strength (GPa)	S_{FC}	0.5
E_Limit		2.5
Delamination factor	S	0.3
Friction angle	φ	20
Strain Rate Coefficient	C	0.024
Tensile fiber damage parameter	AM1	1

Table 2.
Material properties for the tool steel projectile

Density (Kg m^{-3})	ρ	7860
Poisson's ratio	υ	0.28
Yield strength (GPa)	σ_y	1.08
Young's Modulus (GPa)	E	210

Table 3.
Dimensions of quarter symmetry model

1/4 plate	
Length (mm)	50
Width (mm)	50
Layer thickness (mm)	0.68
1/4 projectile	
Radius (mm)	6.35
Length (mm)	13.65

*The strength parameters have been modified by up to +10% to provide the best fit to the V_B of the 16-layer composite plate

4. Results and discussion

4.1 Impact Experiments

Ballistic impact tests were performed on 8, 12, and 16-layers of PP/E-glass composite plates. Four or five samples of each thickness were taken and impacted by a 0.50 caliber flat-ended, cylindrical average projectile of mass 13.40 g ± 0.01g. Initially all the samples were impacted above the ballistic regime, and then impact velocity was decreased to achieve the ballistic limit. Table 4 provides impact results of the samples of different thicknesses in terms of ballistic limit velocities and energy absorption along with the numerical prediction obtained from the simulations.

Table 4. Experimental impact result for the 8, 12, and 16 layer PP/E-glass specimens

Specimen	Number of laminates	Incident velocity (m/s)	Incident kinetic energy (J)	Residual velocity (m s^{-1})	Residual kinetic energy (J)	Energy absorbed (J)	Mean experimental ballistic limit (m s^{-1})	Standard deviation for the ballistic limit (m s^{-1})	Numerical predition of ballistic limit (m s^{-1})
1	8 layers	237.1	376.2	NA*	NA*	376.2	181.3	18.7	179.5
2		226.2	342.2	NA*	NA*	342.2			
3		207.9	289.1	NA*	NA*	289.1			
4		187.1	234.3	63.7	27.1	207.2			
5		186.8	233.5	0.0†	0.0†	233.5			
1	12 layers	260.3	455.3	NA*	NA*	455.3	272.5	26.2	250.0
2		330.4	733.6	179.8	217.3	516.3			
3		321.9	695.7	179.5	216.4	479.2			
4		265.2	472.2	NA*	NA*	472.2			
1	16 layers	332.5	742.5	153.9	159.1	583.5	288.8	31	286.1
2		319.1	683.9	121.3	98.8	585.0			
3		279.5	524.6	0.0‡	0.0‡	524.6			
4		285.3	543.3	0.0‡	0.0‡	543.3			

* False velocity reading (data point not valid), † Partial penetration, ‡ Ballistic limit

4.2 Numerical Results and Discussion

During high velocity impact, the kinetic energy of the projectile is transferred to the plate and absorbed through the various damage mechanisms, thereby increasing the internal energy of the system. LS-DYNA verifies the simulation by conservation of energy of the system. The energy transferred to the composite plate from the projectile can be expressed by Equation 2 as:

An accurate simulation should have very* small HGE (<10% of the peak of the IE) and positive

$$E_{tran} = IE_{plate} + KE_{plate} + HGE_{plate} + KE^{erode} + IE^{erode} + |SLE| \quad (2)$$
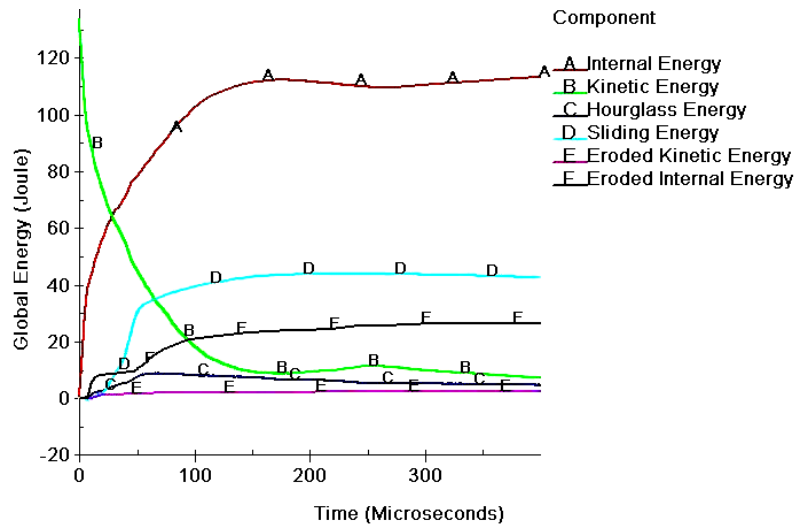

Figure 4: Global energy balance of 16 layer composite laminate at ballistic limit

sliding energy (SLE) which determines perfect global energy balance. Global energy balance of 16-layer composite plate at ballistic limit is shown in Figure 4. Negligible amount of Hourglass (HG) energy mode (curve C) is seen in the Figure. HG modes are nonphysical, zero-energy modes of deformation that produce zero strain and no stress Mesh refinement and proper HG coefficient can reduce hourglassing. In this paper Hourglass type 4 (QM=0.1) was used. Sliding energy (curve D) increases up to 40 because maximum friction is generated at ballistic limit and the kinetic energy (KE) curve decreases to a minimum value at 150 µs indicating that the projectile has come to rest.
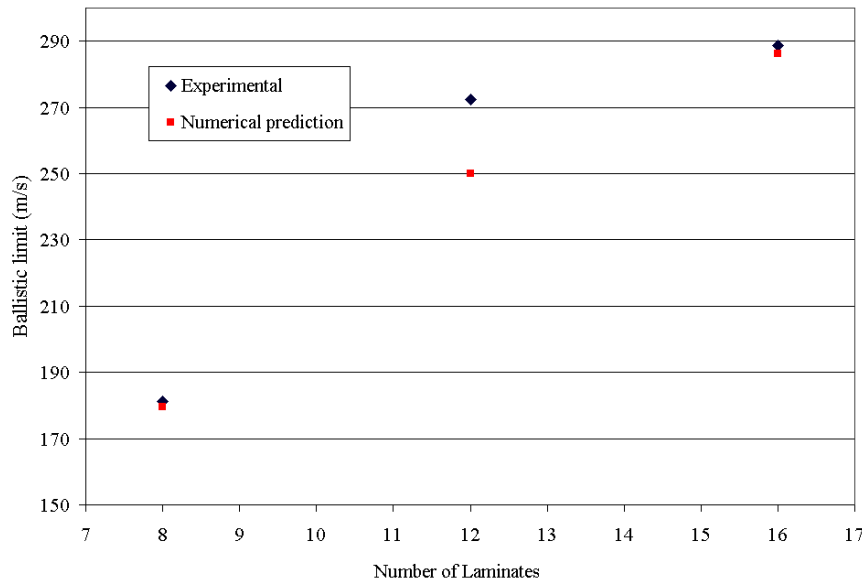

Figure 5. Experimental results and numerical prediction of ballistic limit for the 8, 12 and 16 layer PP/E-glass laminates. The model had an excellent correlation with experimental results for the 8 and 16-layer laminates and a good correlation for the 12-layer laminate at the ballistic limit.

The initial velocities provided to the projectile were identical to those used in the impact tests. Figure 5 depicts the comparison of ballistic limit velocity obtained using simulations with the experimental data. The ballistic limits predicted numerically were found to be in reasonable agreement with the experiment results. There was no erosion or deformation of the projectile during impact.

Figure 6 illustrates the kinetic energy plots of the projectiles with respect to time and corresponding projectile penetrations at different time stages. Damage growth in a single projectile impact can be attributed to the combination of fiber failure modes including punch shear plugging, fiber crush and tension. During impact, a peak stress generates at the contact region and propagates along the primary yarns that are strained to their tensile failure, while secondary yarns undergo elastic deformation [23]. Figure 7 shows fiber failure along the primary yarns of a 12-layer composite laminate for both experimental and numerical conditions respectively. Increase in compliance of the composite plate during impact is one of the major phenomena observed in ballistic impact.
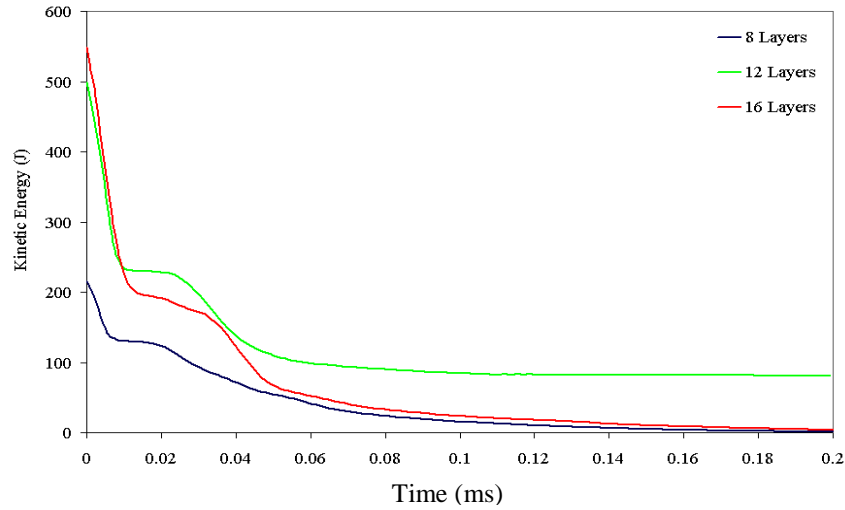
Figure 6: Simulation results showing the kinetic energy lost by the projectile vs. time for the 8, 12, and 16 layer laminates at the experimentally predicted ballistic limit.
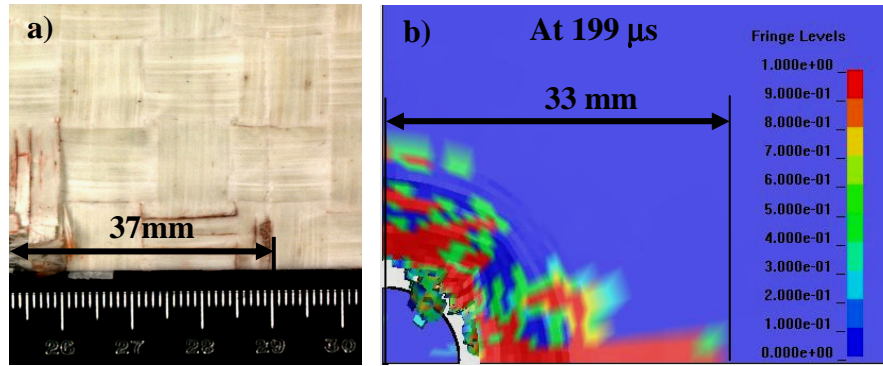

Figure 7: Fiber failure along the primary yarns (X_{11}) of 12 layer plate at V_i=330.4 m s^{-1} (a) experimental (b) simulation

The stiffness (elastic moduli) reduction can be expressed in terms of the associated damage parameters ϖ_i, given by Equation 3.

$$E_{red} = (1 - \varpi_i)E_i \qquad (3)$$

As suggested by Matzenmiller [23], damage variables, ϖ_i grow according to Equation 4:

$$\varpi_i = 1 - e^{\frac{1}{m_i}\left(1 - r_j^{m_i}\right)} \qquad (4)$$

where m_i is the softening parameter. As the damaged zone of each PP/E-glass plate during experimental test was observed to be more localized, $m_i = 0.1$ was used in all the simulations. High strain rate and high pressure loading conditions affect the lamina properties, as denoted by Equation 5:

$$\{S_{eff}\} = \{S_{RT}\}\left(1 + C_1 \ln \frac{\{\dot{\bar{\varepsilon}}\}}{\dot{\varepsilon}_0}\right)^{-1} \qquad (5)$$

Sensitivity analysis on the strain rate parameter, C_1 revealed that a higher value than the range of 0.02-0.05 of C_1 leads to numerical instability. A value of 0.025 was found reasonable maintaining the perfect energy balance. Delamitation at the interface is one of the major failure mechanism at the matrix mode. It is caused by the interlaminer stresses $(\sigma_3, \tau_{23}, \tau_{31})$ due to which matrix microcracks span through the fiber-matrix interface and propagate along the fiber. This leads to subsequent parallel matrix mode failure known as delamination. MAT 161 provides an insight into the physics of the delamination of the composite plate as given by Equation 6:

$$f_{delamination} = S_d\left(\frac{\langle\sigma_3\rangle}{Z_T}\right)^2 + \left(\frac{\sigma_{23}}{S_{yz}}\right)^2 + \left(\frac{\sigma_{31}}{S_{zx}}\right)^2 - 1 \qquad (6)$$

where Z_T, S_{yz} and S_{zx} are the failure strength properties and σ_3, σ_{23} and σ_{31} are corresponding stress state. The delamination scale factor, S_d has a significant effect on ballistic limit velocity or energy absorption of composite plates. S_d is introduced to achieve better correlation of delamination area with experiments by scaling it up and down. The region (marked red, or shown as 35 mm on the scale) in Figure 8 indicates the debonding of the fibers from the surrounding matrix and represents delamination failure of the laminates for both numerical and experimental observation for a 16-layer composite laminate at ballistic limit. As can be seen, the predicted damage is identical to the simulation.
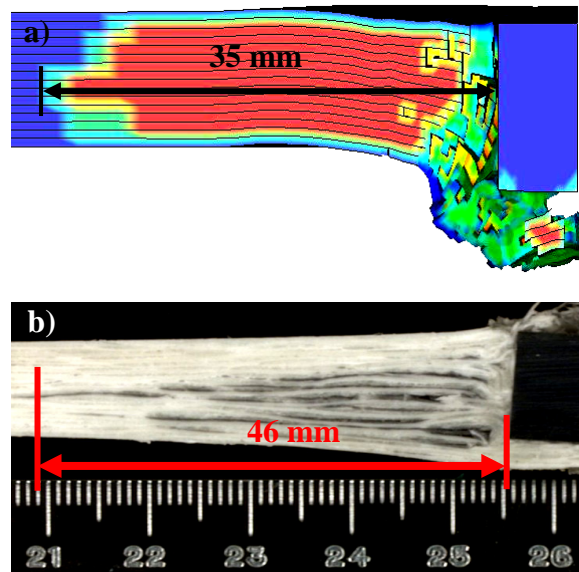

Figure 8. Delaminated area of 16 layer composite at ballistic limit (a) simulation (b) experimental (cross section).

5. Summary

The progressive damage of a composite laminate was investigated using the continuous damage mechanism (CDM) approach suggested by the MLT theory. On the basis of the CDM technique, MAT 161 has been implemented in LS-DYNA. This model was successfully used to analyze the different failure modes of a composite plate subjected to ballistic impact. MAT 161 was used to observe the different damage modes in PP/E-glass, a thermoplastic composite laminate. The ballistic limit and energy absorption of composite laminates of different thicknesses was investigated. It was found that the numerical prediction of ballistic limit velocities of 8, 12 and 16-layer laminates was 99.0%, 92.7% and 99.1% of the corresponding experimental results, respectively. The S_d factor of 0.3 was determined to provide excellent correlation of ballistic limit and delamination failure mode to that observed experimentally. Under the ballistic regime, the effect of boundary conditions has been found to be negligible on the energy absorption of PP/E-glass composite because the damage zone was highly localized and the impact event was transient.

6. References

1. Abrate S., 'Impact on Composite Structures', Cambridge University Press, Cambridge, 1998, UK.
2. Goldsmith W. et al., 'Quasi-static and ballistic perforation of carbon fiber laminates', International Journal of Impact Engineering ,Vol. 32(1), 1995, pp. 89-103.
3. Sun C.T., Potti S.V., 'A simple model to predict residual velocities of thick composite laminates subjected to high velocity impact', International Journal of Impact Engineering, Vol. 18 (3), 1996, pp. 339-353.
4. Morye S. S et al., 'Modeling of the energy absorption by polymer composites under ballistic impact', Composites Science and Technology, Vol. 60, 2000, pp. 2631-2642
5. Department of Defense Test Method Standard V_{50} Ballistic Test for Armor, MIL-STD-662F, DECEMBER 18, 1997.
6. Mines et al., 'High velocity perforation behavior of polymer composite laminates', International Journal of Impact Engineering, Vol. 22, 1999, pp. 561- 588.
7. Lee S. W. R., Sun C. T. 'Dynamic penetration of graphite/epoxy laminates by a blunt-ended projectile', Composite Science and Technology, Vol. 49, 1993, pp. 369-80.
8. Zhu et al., 'Penetration of laminated Kevlar by Projectiles-I, Experimental Investigation', International Journal of Solids Structures, Vol. 29, 4, 1992, pp. 399-421.
9. Zhu et al., 'Penetration of laminated Kevlar by Projectiles-II, Analytical model', International Journal of Solids Structures, Vol. 29, 4, 1992, pp. 421-436.
10. Okafor A.C. et al., 'Detection and characterization of high-velocity impact damage in advanced composite plates using multi-sensing techniques', Composite Structures, Vol. 54, 2001, pp. 289-297.
11. Wen H. M., 'Predicting the penetration and perforation of FRP Laminates struck normally by projectiles with different nose shapes', Composite Structures, Vol. 49, 2000, pp. 321-329.
12. Wen H.M., 'Penetration and perforation of thick FRP laminates', Composite Science and Technology, Vol. 61, 2001, pp. 1163-1172.
13. Abrate A. 'Impact on laminated composites: recent advances', Appl. Mech. REV, Vol. 47, 1994, pp. 517-543.
14. Choi et al., 'Impact damage threshold of laminated composite', in failure criteria and analysis in dynamic response', AMD Vol.107 ASME Applied Mechanics Division, Dallas, TX, November 1990, pp. 31-35.
15. Davis et al., 'Impact damage prediction in carbon prediction composite structures', International Journal of. Impact Engineering, Vol 16, 1995, pp. 149-147.
16. Richarson et al., 'Review of low velocity impact properties of composite materials', Composites, Vol 27 (A), 1996, pp. 1123-1131.
17. Cantwell et al, 'Impact perforation of carbon fiber reinforced plastic', Composite Science and Technology, Vol. 38, 1990, pp. 119-40.
18. Mahfuz et al., 'Investigation of high-velocity impact on integral armor using finite element method', International Journal of. Impact Engineering, Vol. 24, 2000, pp. 203-17.

19. Deluca E et al., 'Ballistic damage impact of S2 glass reinforced plastic structural armor', Composite Science and Technology, Vol. 58, 1998; pp. 1453-61.

20. Johnson A. F. et al., Computational methods for predicting the impact damage in composite structures', Composite Science and Technology, Vol. 61, pp. 2183-2192.

21. Ladevaze P. et al., 'Damage modeling of the elementary ply for laminated composite', Composite Science and Technology, Vol. 43 , pp. 257-267.

22. Allix O., Ladevaze P., 'Interlaminer interface modeling for the prediction of delamination', Composite Structures, Vol. 22, pp. 235-242.

23. Matzenmillar et al., 'A constitutive model for anisotropic damage in fiber composites', Mechanics of Materials, Vol. 20, pp. 125-152.

24. Williams K. V., Vaziri R., 'Application of a damage mechanics model for predicting the impact response of composite materials', Computers and Structures., Vol. 79, pp. 997-1011.

25. Yen Chian-Fong, 'Ballistic impact modeling of composite materials', In: proceedings of the 7th International LS-DYNA Users Conference, Detroit, Michigan, 2002, pp. 15-25.

26. Chan S. et al., 'Ballistic limit prediction using a numerical model with progressive damage capability', Composite Structures (2005) (Article in press).

27. Brown et al., 'Numerical simulation of damage in thermoplastic composite materials', In: proceedings of the 5th European LS-DYNA users conference, Birmingham, UK, May 25-26, 2005.

28. Hashin Z. 'Failure criteria for unidirectional fiber composites', Journal of Applied Mechanics, Vol. 47, 1980, pp. 329-334.

29. LS-DYNA Theoretical Manual, version 950, Livermore Software Tech. Corp., May 1998